Adiabatic potential-energy surfaces for higher excited states of the H_2^+ ion in a strong magnetic field

U. Kappes and P. Schmelcher
Theoretische Chemie, Physikalisch-Chemisches Institut, Im Neuenheimer Feld 253, 69120 Heidelberg, Federal Republic of Germany
(Received 18 March 1996)

We investigate the topology of the adiabatic potential-energy surfaces of the $4_{g\,(u)}$,$5_{g\,(u)}$,$6_{g\,(u)}$ electronic states of the hydrogen molecular ion in a strong magnetic field. The increasing complexity of the surfaces with increasing degree of electronic excitation is demonstrated. Stable local as well as global molecular equilibrium configurations are found for the parallel, perpendicular, as well as intermediate configurations. [S1050-2947(96)01108-0]

PACS number(s): 33.15.−e, 33.55.Be

The behavior and properties of atoms and molecules in strong magnetic fields have become, in the past 20 years, a field of intense research. On the one hand, this was motivated by the discovery [1] of huge field strengths (10^2–10^8 T) in the atmosphere of astrophysical objects such as white dwarfs and neutron stars and, on the other hand, highly excited atomic or molecular Rydberg states became accessible at laboratory field strengths of a few tesla both theoretically as well as experimentally. Compared to the field-free situation, the external magnetic field induces a strong change of the electronic structure of these systems. For molecules there exist several investigations on the low-lying electronic states of the hydrogen molecular ion H_2^+ at astrophysical field strengths that reveal a number of interesting phenomena and effects (see Refs. [2–6] and references therein). In the first few investigations it was realized that the dissociation energy for the ground state of the ion increases rapidly with increasing field strength. The overall size of the molecule hereby decreases significantly due to the more complete screening of the nuclear charges. Recent investigations [5] showed the existence of two classes of excited electronic states of the H_2^+ ion that are unbound in field-free space and become bound, i.e., stable, above some critical field strength and are even more strongly bound in the high-field regime.

In the presence of a magnetic field the adiabatic electronic potential energies depend, already for a diatomic molecule, on the internuclear distance R as well as the angle Θ between the internuclear and magnetic-field axes, i.e., they are two-dimensional surfaces. In a very recent work [6] the local as well as global topological properties of the surfaces belonging to the three lowest electronic states of gerade and ungerade parity have been investigated. A variety of different possibilities for the topological behavior of the adiabatic potential-energy surfaces (PESs) have been derived and discussed. In particular it has been shown that local as well as global equilibrium configurations of the ion occur not only for the positions with higher symmetry (see below), i.e., for the parallel and perpendicular positions, but also for configurations that correspond to an inclination of the internuclear axis with respect to the external field. An example for the latter case is the PES of the 3_u electronic state, which exhibits its global minimum at $\Theta=27°$.

The subject of the present paper is to investigate the behavior and properties of the PES for higher excited states of the H_2^+ ion in a strong magnetic field. Specifically we will study the topology of the 4_g,5_g,6_g and 4_u,5_u,6_u excited adiabatic electronic states, which will give us an idea of the enormously increasing complexity of the spectrum of molecules in external fields with increasing excitation.

Before entering the discussion of the results of our extensive computation on the hydrogen molecular ion we briefly comment on some of the general properties of the adiabatic electronic states and their PESs in the presence of a strong magnetic field. The molecular symmetry point groups of the fixed-nuclei Hamiltonian [7] for a diatomic molecule in a magnetic field depend strongly on the orientation of the internuclear axis with respect to the magnetic field. For the parallel configuration of a homonuclear diatomic molecule the symmetry point group is $C_{\infty h}$, whereas the orthogonal configuration possesses the C_{2h} symmetry group. For arbitrary values of the angle Θ only parity is conserved, i.e., we obtain the inversion group C_i. The parallel and orthogonal configurations are therefore distinguished by their higher symmetry. Two PESs that possess different symmetries at either $\Theta=0°$ or 90° are allowed to cross each other without interacting at $\Theta=0°$ or 90°, respectively. If the two PESs possess the same parity, these crossings turn into avoided crossings if we incline the internuclear axis with respect to its parallel or orthogonal position. The common manifold of the intersecting PESs is therefore a conical intersection point. The avoided crossings for $\Theta=0°$,90° are a consequence of the noncrossing rule [8], which holds for our case of a complex Hermitian eigenvalue problem with equal parity states.

Our electronic-structure calculations have been performed using a generalized atomic orbital basis set [9], which has been optimized recently [10]. The typical number of atomic orbitals we used throughout our calculations was roughly 360. In spite of the excellent convergence properties of the corresponding symmetry-adapted molecular orbitals, our computations for the higher excited PESs were very time consuming. A large number of grid points in (R,Θ) space was necessary in order to construct each PES. The total CPU time of our large-scale computations amounts to $1\frac{1}{2}$ years on an R4000 Silicon Graphics workstation. For details of the numerical method as well as the computational techniques we refer the reader to the literature [5,9,10]. We remark that throughout the paper we will use atomic units.

In the following we consider the higher excited adiabatic

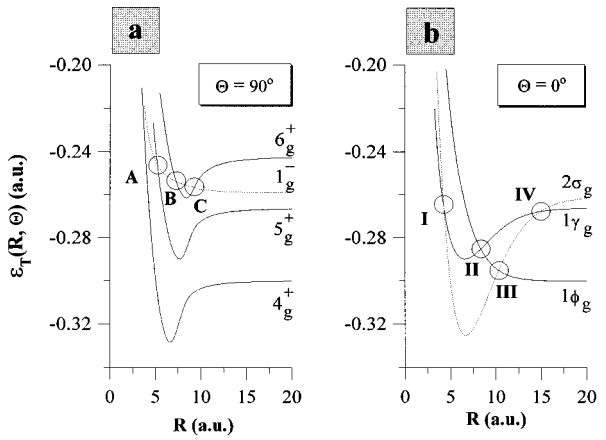

FIG. 1. Potential-energy curves belonging to the intersections of the total electronic energies $\epsilon_T(R,\Theta)$ at (a) $\Theta=90°$ and (b) $\Theta=0°$ of the 4_g,5_g,6_g adiabatic electronic states. The labels $A-C$ and I–IV indicate conical intersection points of the corresponding surfaces.

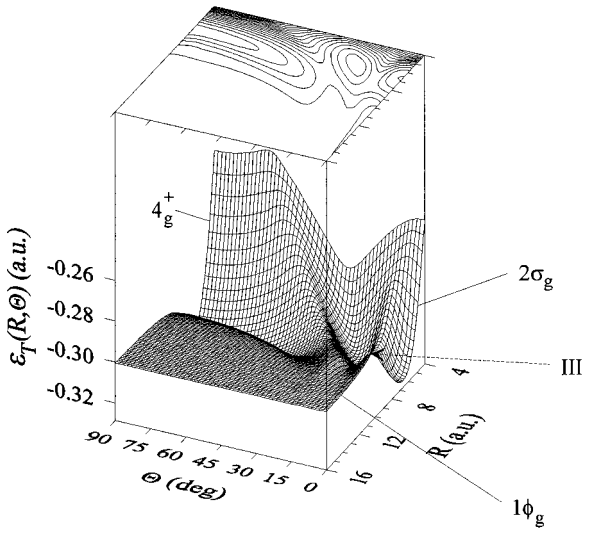

FIG. 2. Electronic PES $\epsilon_T(R,\Theta)$ and the corresponding contour plot of the 4_g electronic state. The global minimum of the PES is located at $\Theta=90°$, $R=6.62$ and has a dissociation energy $\epsilon_D=2.859\times10^{-2}$. In addition there exist two local minima at $\Theta=0°$ and 21°. The label III indicates the conical intersection point with the upper 5_g surface.

$4_{g\,(u)}$,$5_{g\,(u)}$,$6_{g\,(u)}$ electronic states of the hydrogen molecular ion embedded in a typical strong field $B=1.0$ a.u. ($\approx2.35\times10^5$ T). Let us begin our discussion with the electronic states of gerade parity for the two positions $\Theta=0°$ and 90° distinguished by symmetry. Figure 1(a) illustrates the intersections of the PESs, i.e., the potential-energy curves (PECs) for the 4_g,5_g,6_g electronic states at $\Theta=90°$. The PEC of the energetically lowest 4_g surface is well separated from the PECs of the higher excited states and belongs to the single electronic 4_g^+ state. In contrast to this, the PECs of the 5_g,6_g PESs at $\Theta=90°$ are composite and exhibit a number of crossings that are indicated in Fig. 1(a) through the encircled regions labeled by A, B, and C. The PEC of the 5_g surface at $\Theta=90°$ belongs, for small internuclear distances, to the 1_g^- electronic state and for larger internuclear distances to the 5_g^+ state. The crossing of the corresponding PEC is located in their repulsive part, i.e., far from any equilibrium internuclear distances. This crossing turns into an avoided crossing if we rotate the internuclear axis from the perpendicular configuration. In the two-dimensional (R,Θ) space we therefore encounter a conical intersection of the 5_g and 6_g PESs at $\Theta=90°$ and for $R\approx5.2$. Finally, the PEC of the 6_g PES at $\Theta=90°$ belongs to three different electronic states. With increasing internuclear distance we encounter the 5_g^+,1_g^-,6_g^+ states and for large internuclear distances again the 1_g^- electronic state. This implies a total number of three crossings, i.e., conical interactions of the corresponding surfaces, which are indicated in Fig. 1(a) by the encircled regions A, B, and C.

Next let us consider the intersections, i.e., PECs, for the PESs of the 4_g,5_g,6_g electronic states at $\Theta=0°$, which are illustrated in Fig. 1(b). The PEC for the energetically lowest 4_g surface consists of two major parts. Apart from the crossing in the strongly repulsive regime indicated by the label I in Fig. 1(b), this PEC belongs, for $4.0<R<10.1$, to the $2\sigma_g$ electronic state and, for $R>10.1$, to the $1\Phi_g$ state. We encounter, therefore, two conical intersections of the lower 4_g and upper 5_g surfaces at $\Theta=0°$, which are indicated in Fig. 1(b) by the encircled regions labeled by I and III. The 5_g PES possesses, in addition, at $\Theta=0°$ two conical intersections with the upper 6_g PES, which are indicated in the PEC of Fig. 1(b) by the encircled regions II and IV. The PEC of the 5_g PES at $\Theta=0°$ belongs, for $4.0<R<8.1$, to the $1\gamma_g$ state, for $8.1<R<10.1$ to the $1\Phi_g$ state, for $10.1<R<14.7$ to the $2\sigma_g$ state, and for $R>14.7$ again to the $1\gamma_g$ state. Finally, the 6_g PES exhibits, of course, also the conical intersections with the lower 5_g PESs indicated as II and IV in Fig. 1(b) and its PEC in Fig. 1(b) belongs within the displayed coordinate range to the $1\Phi_g$,$1\gamma_g$ and for large internuclear distances to the $2\sigma_g$ adiabatic electronic states.

After having discussed the properties of the PEC belonging to the PES with gerade parity at the configurations $\Theta=0°$ and 90°, we study, in the following, the local as well as global topological properties of the corresponding complete surfaces. Let us begin with the 4_g surface. Figure 2 illustrates the 4_g PES in (R,Θ) space together with the corresponding contour plot. It possesses three minima with well-pronounced potential wells. Two of them are located at the positions distinguished by symmetry, i.e., $\Theta=0°$,90°, and the third minimum is located at $\Theta=21°$, i.e., at a position of lower symmetry (remember that inversion is the only symmetry left for $\Theta\neq0°$,90°). The corresponding internuclear distances are 6.64, 6.62, and 6.25, respectively. The dissociation energies belonging to the potential wells of these minima are 2.539×10^{-2}, 2.859×10^{-2}, and 2.300×10^{-2}, respectively. The global minimum of the 4_g PES is therefore located at $\Theta=90°$. The potential well around the minimum at $\Theta=21°$ is well separated from the lower 3_g surface (the minimal energetic distance is 2.839×10^{-2}) as well as the upper 5_g surface. The PES of the 4_g electronic state is therefore a nice example for a surface that exhibits all three qualitatively different kinds of minima and potential wells. In particular vibronic interaction does not play a crucial role for the low-lying vibrational states in these wells. The only conical intersection point of the 4_g with the 5_g PESs at ($R=10.1$, $\Theta=0°$), indicated in Fig. 2 by the label III [see also Fig.

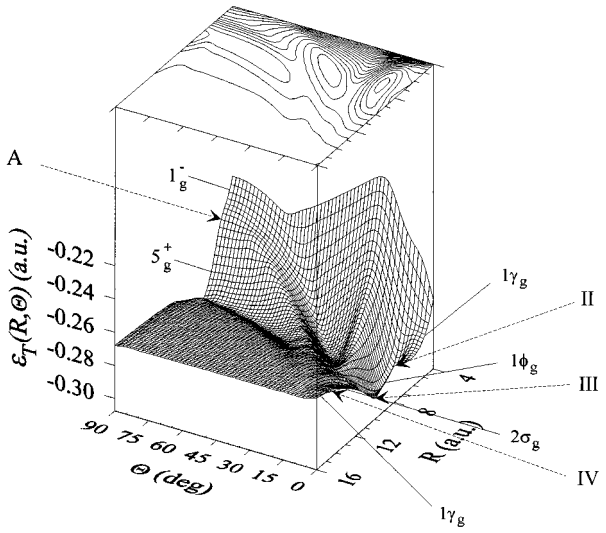

FIG. 3. Electronic PES $\epsilon_T(R,\Theta)$ and the corresponding contour plot of the 5_g electronic state. The global minimum of the PES is located at $\Theta=9°$, $R=7.5$ and possesses a dissociation energy $\epsilon_D=4.153\times10^{-2}$. The two other local minima occur for $\Theta=90°$ and 33°. At $\Theta=0°$ we encounter three conical intersection points labeled II, III, and IV. The perpendicular configuration shows only one conical intersection *A* in the strongly repulsive part of the corresponding potential-energy curve.

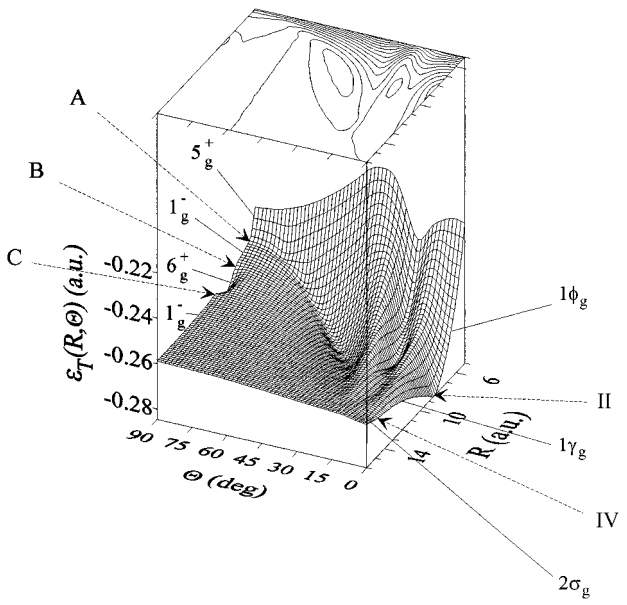

FIG. 4. Electronic PES and the contour plot of the 6_g state. The global minimum occurs for $\Theta=40°$, $R=8.5$ with a dissociation energy $\epsilon_D=1.4\times10^{-2}$. A local minimum occurs for $\Theta=16°$, $R=8.5$. At $\Theta=0°$ we encounter two conical intersection points labeled II and IV. The intersection point II is located at the bottom of the well around $\Theta=0°$. For $\Theta=90°$ we have three conical intersection points *A*, *B*, and *C*.

1(b)], is located far from the stable vibrational configurations.

Next let us consider the PES of the 5_g state, which is illustrated together with the corresponding contour plot in Fig. 3. This surface possesses also three minima, but only one of them is located at a position distinguished by symmetry, i.e., at $\Theta=90°$. The two other minima are located at $\Theta=9°$ and 33°. The corresponding internuclear equilibrium distances are 7.66, 7.50, and 7.10, respectively. Around the minima we encounter well-pronounced potential wells of different elliptical shape, which can clearly be seen in Fig. 3. The dissociation energies are 2.376×10^{-2}, 4.153×10^{-2}, and 2.813×10^{-2}, respectively. The global minimum of the 5_g PES is therefore located at $\Theta=9°$, i.e., at a position that possesses low symmetry. The 4_g and 5_g surfaces possess the smallest distance, i.e., come closest to each other in the immediate neighborhood of the minima located at $\Theta=9°$ and 33°. The energetical distance of the 4_g and 5_g PESs at the minimum $\Theta=9°$ of the 5_g surface is $\Delta\epsilon=3.955\times10^{-3}$ and at the minimum $\Theta=33°$ we have $\Delta\epsilon=1.065\times10^{-2}$. The occurrence of the minima at $\Theta\neq0°,90°$ is at least partially a consequence of the repulsion of the PES due to the noncrossing rule. With increasing degree of excitation, the number of avoided crossings, and therefore also the number of potential wells located at $\Theta\neq0°,90°$, increases rapidly. The conical intersection points of the 5_g PES mentioned in the discussion of Fig. 1 (see above) are indicated in Fig. 3 with II, III, and IV for the perpendicular configuration and with *A* for the parallel configuration.

Finally, Fig. 4 shows the PES and its contour plot of the 6_g electronic state. It possesses two well-pronounced potential wells for $\Theta\neq0°,90°$. The corresponding minima are located at ($R=8.5$, $\Theta=16°$) and ($R=8.5$, $\Theta=40°$). The dissociation energies are 1.25×10^{-2} and 1.4×10^{-2}, respectively. The two wells are separated by a potential barrier that is energetically much higher than the corresponding dissociation energies. The low-lying vibrational states in these two-dimensional wells represent stable molecular configurations. The well located at $\Theta=16°$ is separated by another potential barrier from a third well located at $\Theta=0°$. The latter well contains, however, no vibrationally stable states because of the conical intersection II of the 6_g and 5_g surfaces, which is located at the minimum of this well. The 6_g PES possesses, at $\Theta=90°$, according to the discussion of Fig. 1(a) (see above), three conical intersections with the lower 5_g surface. The $\Theta=90°$ configuration is not a stable molecular configuration for the 6_g excited electronic state.

In the following we discuss the properties of the PESs belonging to the electronic states with ungerade parity. The PESs belonging to the gerade and ungerade states cross each other without interacting. First of all, we again restrict ourselves to the positions of distinguished symmetry, i.e., we consider the PECs for the positions $\Theta=0°$ and 90°. Figure 5(a) shows the intersections, i.e., PECs, of the 4_u,5_u,6_u PESs for the perpendicular configuration $\Theta=90°$. The PEC of the lowest 4_u PES at $\Theta=90°$ belongs, for arbitrary internuclear distance, to the 4_u^+ state and is energetically well separated from all other PECs. In contrast to this, the PEC of the 5_u PES at $\Theta=90°$ belongs, for $R<6.2$, to the 1_u^- state and, for $R>6.2$, to the 5_u^+ state. The transition point represents a conical intersection point of the upper 6_u surface with the lower 5_u surface. It is indicated in Fig. 5(a) by the encircled region with the label *A*. On the other hand, the PEC of the upper 6_u surface at $\Theta=90°$ belongs, for $R<6.2$, to the 5_u^+ and, for $R>6.2$, to the 1_u^- state.

Next let us turn to the intersections, i.e., PECs, at $\Theta=0°$, which are illustrated in Fig. 5(b). The PEC of the 4_u surface

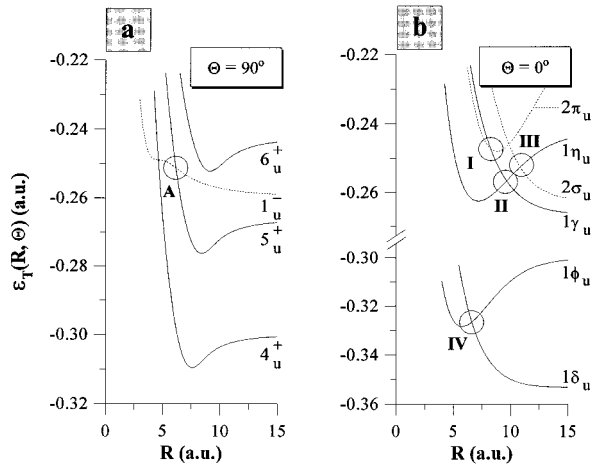

FIG. 5. Potential-energy curves belonging to the intersections of the total electronic energies $\epsilon_T(R,\Theta)$ at (a) $\Theta=90°$ and (b) $\Theta=0°$ of the 4_u,5_u,6_u adiabatic electronic states. The labels *A* and I–IV indicate conical intersection points of the corresponding surfaces.

at $\Theta=0°$ belongs, for $R<6.7$, to the $1\delta_u$ state and, for $R>6.7$, to the $1\phi_u$ state. The transition point represents a conical intersection point of the lower 3_u PES with the 4_u PES and is indicated in Fig. 5(b) by the encircled region labeled IV. The PEC of the 5_u PES at $\Theta=0°$ belongs, for $R<9.8$, to the $1\eta_u$ state and, for $R>9.8$, to the $1\gamma_u$ state. The conical intersection point II is the point where the upper 6_u surface touches the 5_u PES. The decomposition of the PEC of the 6_u PES at $\Theta=0°$ is more complicated. For small internuclear distances $R<8.3$ it belongs to the $2\pi_u$ electronic state, for $8.3<R<9.8$ to the $1\gamma_u$ state, for $9.8<R<10.7$ to the $1\eta_u$ state, and for $R>10.7$ to the $2\sigma_u$ state. These four different parts of the PEC are separated by three conical intersection points labeled in Fig. 5(b) with I, II, and III. The intersection points I and III correspond to intersections with energetically even higher excited PESs, whereas the intersection point II belongs, as already mentioned above, to the intersection of the 5_u,6_u surfaces.

We turn now towards a discussion of the topology of the two-dimensional PESs for the 4_u,5_u,6_u electronic states. Figure 6 illustrates the PES for the 4_u state in (R,Θ) space together with its contour plot. The surface exhibits three minima. Two of them are located at the positions $\Theta=0°$,$90°$ of higher symmetry and the third minimum occurs for $\Theta=35°$. The corresponding internuclear distances are

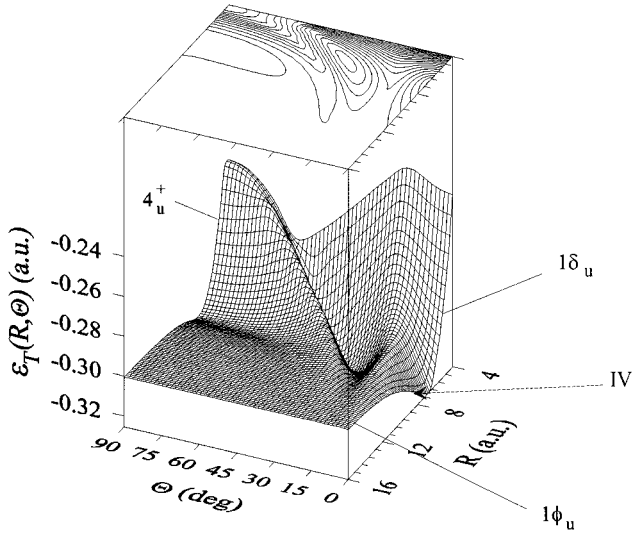

FIG. 6. Electronic PES and the contour plot of the 4_u state. The surface possesses three minima: a shallow well around $\Theta=90°$, $R=7.57$, a second deeper well around $\Theta=35°$ with $\epsilon_D=2.274\times10^{-2}$, and the global minimum at $\Theta=0°$ and $R=6.7$, which is, however, unstable due to the conical intersection with the lower 3_u surface.

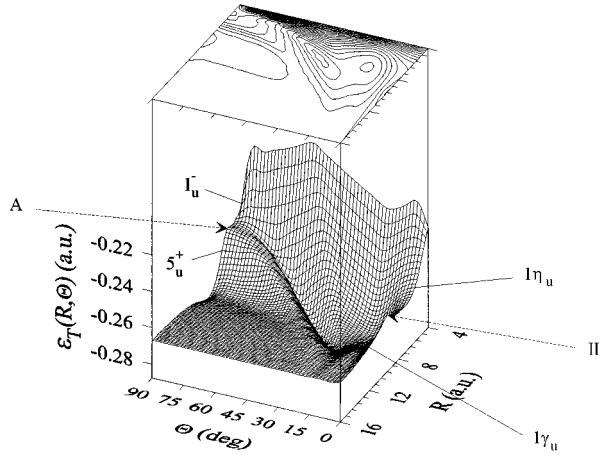

FIG. 7. Electronic PES and the corresponding contour plot of the 5_u state. There exist two minima with well-pronounced potential wells at $\Theta=39°$, $R=7.65$ and $\Theta=90°$, $R=8.41$. In addition, we have a shallow well at $\Theta=15°$. *A* and II are the conical intersections with the upper 6_u PES.

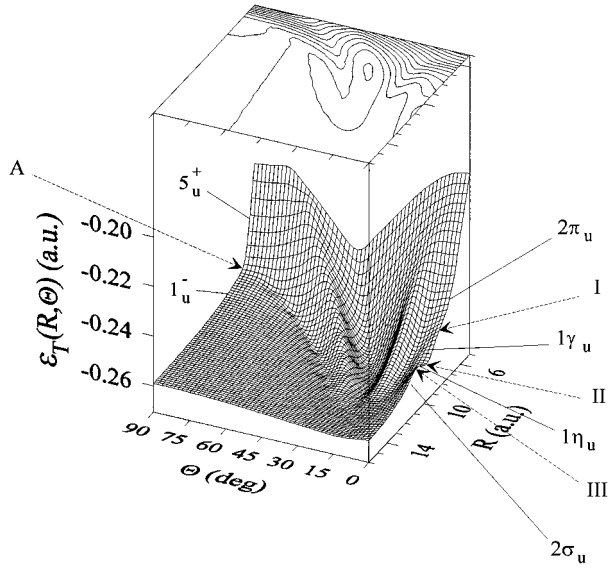

FIG. 8. Electronic PES and the corresponding contour plot of the 6_u state. There exists one well-pronounced potential well around the minimum at $\Theta=30°$, $R=8.25$ with a dissociation energy $\epsilon_D=10^{-2}$. I, II, and III indicate the intersection points at $\Theta=0°$ and *A* is the only intersection point for the purely repulsive PEC at $\Theta=90°$.

$R=6.7$, 7.57, and 6.4, respectively. The depths (dissociation energies) of the three underlying potential wells are 2.615×10^{-2}, 0.968×10^{-2}, and 2.274×10^{-2}. The global minimum is therefore located at $\Theta=0°$. However, this minimum is given by the conical intersection IV of the 3_u and 4_u PESs at $\Theta=0°$ (see also the discussion above). A wave packet located in the potential well at $\Theta=0°$ of the upper 4_u surface will, due to vibronic interaction, decay rapidly to the lower 3_u surface. The global minimum including the requirement of stability is therefore the minimum at $\Theta=35°$.

Next let us discuss the PES of the 5_u state, which is shown in Fig. 7 together with the corresponding contour plot. This surface possesses minima with well-pronounced potential wells at ($R=7.65$, $\Theta=39°$) and ($R=8.41$, $\Theta=90°$). The corresponding dissociation energies are 2.148×10^{-2} and 1.018×10^{-2}, respectively. The global minimum is therefore located at $\Theta=39°$, i.e., just above the ridge of the lower 4_u PES. Indeed, the energetic distance of these two surfaces is particularly small (5.771×10^{-3}) at the position of the global minimum of the 5_u PES, which indicates the importance of vibronic interaction for the formation of this minimum. In addition, there exists a very shallow minimum or structure located at ($R=7.5$, $\Theta=15°$) with a depth of 2×10^{-3}. The PES of the 5_u state exhibits two conical intersections: one at $\Theta=90°$, shown in Fig. 7 by the label *A*, and one at $\Theta=0°$, indicated by the label II (see, in particular, also the discussion of the intersections at $\Theta=0°$,90° above).

Finally, Fig. 8 illustrates the PES of the 6_u electronic state. According to the discussion of Figs. 5(a) and 5(b), we encounter three conical intersections with the PES of the 5_u electronic state at $\Theta=0°$ (labeled I, II, and III in Fig. 8) and one conical intersection (labeled *A*) at $\Theta=90°$. The parallel and perpendicular configurations do not correspond to stable molecular configurations for the 6_u electronic state. Apart from a very shallow channel, the 6_u PES possesses a potential well around the minimum located at ($R=8.15$, $\Theta=30°$) and with a dissociation energy of approximately 10^{-2}. This well extends far in the direction of increasing internuclear distance and contains vibrationally stable states.

The Deutsche Forschungsgemeinschaft is gratefully acknowledged for financial support.

[1] J. P. Ostriker and F. D. A. Hartwick, Astrophys. J. **153**, 797 (1968); J. Kemp, J. S. Swedlund, J. Landstreet, and J. Angel, *ibid.* **161**, L77 (1970); J. Trümper, W. Pietsch, C. Reppin, B. Sacco, E. Kendziorra, and R. Staubert, Ann. N. Y. Acad. Sci. **302**, 538 (1977).

[2] D. M. Larsen, Phys. Rev. A **25**, 1295 (1982).

[3] D. R. Brigham and J. M. Wadehra, Astrophys. J. **317**, 865 (1987).

[4] U. Wille, Phys. Rev. A **38**, 3210 (1988).

[5] U. Kappes and P. Schmelcher, Phys. Rev. A **50**, 3775 (1994); **51**, 4542 (1995).

[6] U. Kappes and P. Schmelcher, Phys. Lett. A **210**, 409 (1996); Phys. Rev. A **53**, 3869 (1996).

[7] P. Schmelcher and L. S. Cederbaum, Phys. Rev. A **41**, 4936 (1990); P. Schmelcher, L. S. Cederbaum, and U. Kappes, in *Conceptual Trends in Quantum Chemistry* (Kluwer Academic, Dordrecht, 1994), pp. 1–51.

[8] J. von Neumann and E. Wigner, Phys. Z. **30**, 467 (1929).

[9] P. Schmelcher and L. S. Cederbaum, Phys. Rev. A **37**, 672 (1988).

[10] U. Kappes and P. Schmelcher, J. Chem. Phys. **100**, 2878 (1994).